The International Journal of Advanced Manufacturing Technology (2019) 101:1133–1141
https://doi.org/10.1007/s00170-018-3003-9

ORIGINAL ARTICLE

Studying the effects of cutting parameters on burr formation and deformation of hierarchical micro-structures in ultra-precision raster milling

Wei Zhao[1] · Haitao Wang[1] · Wei Chen[1]

Received: 18 May 2018 / Accepted: 6 November 2018 / Published online: 14 November 2018

Abstract
Hierarchical micro-structures are composed of a primary micro-structure and secondary micro V-grooves (SMVGs) cut by the UPRM one-step method. The key problem is the existence of burrs and plastic deformation of the top of SMVGs during the fly cutting process. This paper presents a study of the burr and deformation information introduced by one-step cutting operation in ultra-precision raster milling (UPRM). A series of experiments was carried out to investigate the effect of cutting conditions on the quality of hierarchical micro-structures by the one-step cutting method. A single point diamond tool with a 40° tool angle was employed to perform the one-step cutting operation in UPRM. Hierarchical micro-structures were produced on copper material successfully. Large burrs and plastic deformation were formed when cutting with a fixed tool angle. These large burrs and deformation were found to be induced by cutting force and cutting parameters. It was found that large burrs are formed with an increase of the cutting depth, feed rate, and spindle speed; the plastic deformations become serious with an increase of the cutting depth and feed rate, but are reduced with a decrease of spindle speed. An experimental study was established to investigate cutting force as a function of the cutting conditions in relation to micro-burr formation in machining, and explore the problems associated with one-step fly cutting in UPRM. The mechanisms of burrs and plastic deformation of SMVGs are discussed to further improve the machining process.

Keywords Hierarchical micro-structure · Ultra-precision raster milling · Burr formation · Plastic deformation

1 Introduction

In the field of heat transfer enhancement, compared to the other single-level micro-structures in a micro heat exchanger, the hierarchical ribs with asymmetric arc geometry and attached SMVG minimize the pressure drop as well as further enhance the heat transfer [1, 2]. SMVGs are important features in increasing the wet area and generating turbulence near the internal wall of a micro heat exchanger as shown in Fig. 1.

Burrs left on the top of micro-grooves are extremely harmful to the performance of the enhancement of heat exchange, due to burrs blocking the valley of V-grooves [3]. In fabrication, burrs also greatly influence the machined surface. In addition, burrs also cause tool wear due to hitting the cutting edge, which results in tool wear. This groove wear, in turn, accelerates burr growth [4].

Since burrs and deformation are always associated with micro-groove machining, many deburring methods have been investigated in micro cutting processing. Liu et al. [5] developed a model which considers two-dimensional (2D) deformation of burrs fully formed by cutting a ductile work material, so that all forces are considered to be distributed per unit width. The effects of the cutting parameters were studied and cutting strategies of burr minimization are discussed. The proposed minimization was achieved by optimizing the cutting conditions, such as cutting speed (Vc), feed per tooth (f_z), and depth of cut (DoC) [6, 7].

The effect of the tool rake angle, workpiece angle and under formed chip thickness on burr dimensions was studied in experiments. The experiments showed that the size of the

✉ Haitao Wang
wanghaitao@szpt.edu.cn

[1] The School of Mechanical and Electrical Engineering Shenzhen Polytechnic, Shenzhen, Guangdong, China

minimum chip thickness has a great influence on the cutting process [8–10]. Burr formation is more complicated when compared to macro cutting. Bissacco [11] and Schueler [12] reported that the top burr size is large in micro-milling due to the size effect.

Some previous studies have focused on the surface generation of UPRM taking cutting force into consideration. To et al. [13] developed a cutting force model to predict the cutting force components both in the feed direction and thrust direction, and a dynamic model was developed to simulate the free vibration signal induced by the cutting force pulse. Parsa et al. [14] proposed that material spring back is the main source of normal force in the orthogonal cutting process. Wang et al. [4] developed a cutting force model based upon the characteristics of the force system and tool geometry, in which the forces acting on the rake face, the cutting edge, and the clearance face of the diamond tool were investigated. However, there has been a lack of comprehensive investigation of the process factors affecting the quality of SMVGs by one-step cutting. As a result, there is a need for analysis of the effect of the cutting factors and the cutting force on the SMVG generation in UPRM. In addition, the relationship between the cutting conditions and cutting force need to be established.

The hierarchical structure features a first-order asymmetric arc rib imposed by SMVGs. Compared to the conventional micro-groove machining method, the hierarchical structure is more complex. The high-quality profile of the first-order structures is required as well as SMVGs. Especially, in order to improve the efficiency of generation, the one-step machining method is employed, which requires that both the first- and second-order structures be completed simultaneously. Guo et al. applied vibration-induced micro-textures to generate hierarchical structures in a one-step machining process. Elliptical vibrations were used to generate the first-order micro-channels in a grooving operation. The second-order textures were simultaneously formed by the overlapping tool trajectories in consecutive vibration cycles. The required wavelength of the second-order micro-textures was determined by the nominal feed velocity [15]. To et al. proposed a virtual spindle-based tool servo diamond turning method to effectively generate second-order discontinuous arrays on freeform surfaces. During the machining process, the first-order freeform surface is generated by essentially splicing the secondary micro-structures obtained through the virtual spindle-based tool servo diamond turning [16]. However, the existing generation methods for hierarchical structures are still limited in terms of discussion of the quality of second-order micro/nano-structures, such as burr information and deformation.In this paper, studies of cutting parameters on the quality of SMVGs fabricated by the one-step process in UPRM processing are considered. Also,

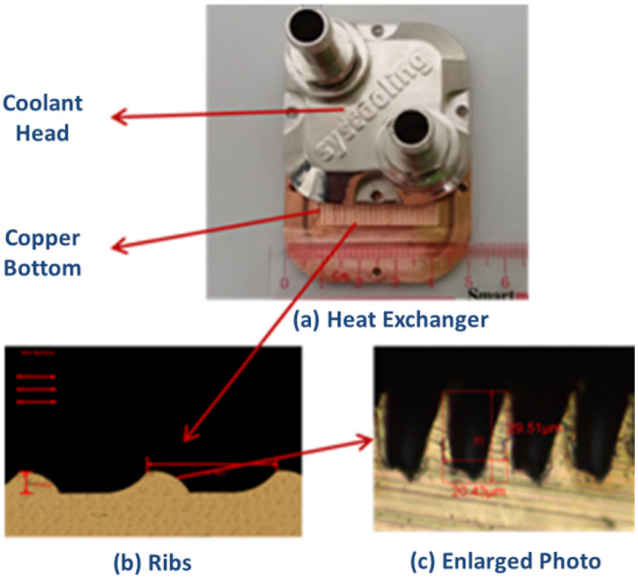

Fig. 1 Photographs of (**a**) a heat exchanger with a detachable bottom plate; (**b**) the hierarchical micro-structure in cross-sectional view; and (**c**) the SMVGs of a hierarchical micro-structures in the enlarged view [2]

through analysis of the cutting parameters such as depth of cut, spindle speed, and feed rate, a dynamic model to relate the burrs and deformation induced by cutting force was established and the relationship between the cutting factors and cutting force investigated. A series of cutting experiments was conducted to estimate the cutting force effect on the quality of SMVGs. The results can be used to explain the basic mechanism of burrs and deformation during the cutting process.

2 Experimental setup

In this study, a series of cutting experiments was carried out. Figure 2 shows a Freeform 705G (Precitech Inc., USA), which was used to fabricate the non-rotational symmetric structure with a nanometer surface finish and submicron form error

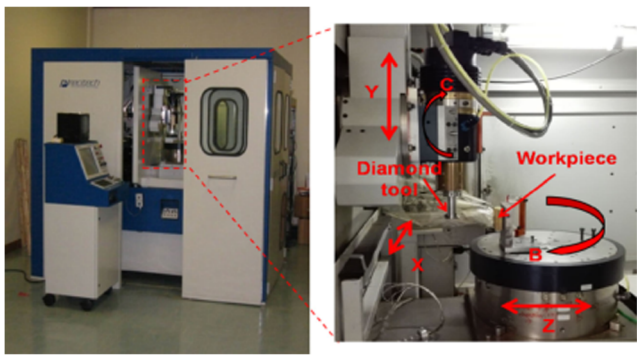

Fig. 2 Freeform 705G ultra-precision machine and five axes of the machine tool

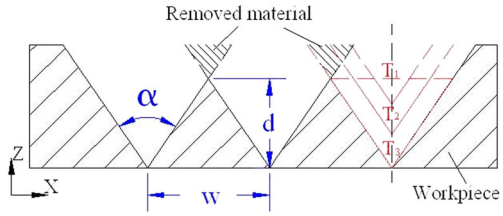

Fig. 3 The mechanism of the volume of removal material for each cutting step

without any further polishing. Regarding the linear axis and spindle motion of the machine, there are three linear axis (X, Y, Z) movements and two rotational axis (B, C) movements. The diamond tool is attached to the spindle. The workpiece is clamped on the fixture and follows the linear motion along the *Y*-axis and rotational motion. The machine performs high-accuracy for three-dimensional milling, grinding, and two-axis turning.

The mechanism of surface generation by ultra-precision raster milling has been discussed in previous papers [3].

The mechanism of each cutting step for generation of micro-grooves is shown in Fig. 3. The red characters (i.e., $\boldsymbol{T_1}$, $\boldsymbol{T_2}\ldots\boldsymbol{T_n}$) represent the order of the cutting steps with a given cutting depth of ε, and the subscript *n* is for cutting times to generate a desired depth of groove. Based on the relationship of step distance *w*, desired micro-groove distance *d* and cutting tool angle α, there are three situations of horizontal cutting. The ideal depth of desired micro-grooves can be calculated by:

$$w = 2d\tan\frac{\alpha}{2} \tag{1}$$

where *d* is the desired depth of micro-grooves, *w* is the step distance, and α is the tool angle. In the cutting process, the tool angle α does not change. According to Eq. (1), if the step distance *w* is kept constant, the depth of SMVGs is always a constant value.

Table 1 Major cutting parameters in UPRM machining experiments

Feed rate *f*	Spindle speed *ω*	Depth of cut *d*	Swing radius *R*	Tool angle
50 mm/min	2000 rpm	2 μm	25.3 mm	40°
100 mm/min	4000 rpm	5 μm		
150 mm/min	6000 rpm	8 μm		

The experiments conducted in the present study further validate the effect of the machining parameters and cutting strategy on the quality of SMVGs. In this paper, three main machining parameters for ultra-precision raster milling are discussed, which are cutting depth (*d*: μm), feed rate (*f*: mm/min), and spindle speed (*ω*: rpm).

2.1 Cutting force modeling

Examples of the machined cross-section of hierarchical structures and cutting force model are given in Fig. 4. The SMVGs overlap on the first-order asymmetric rib surface as shown in the Fig. 4a. These surface features greatly contribute to the enhancement of the heat transfer rate and minimization of the pressure drop in channel flow.

In UPRM, the diamond tool rotates circularly around the spindle axis of the machine tool. When taking the diamond tool as the research object in the cutting process, it is found that the diamond tool suffer from several force components during the cutting process. Because the purpose of this paper is to study the effect of cutting force on the plastic deformation

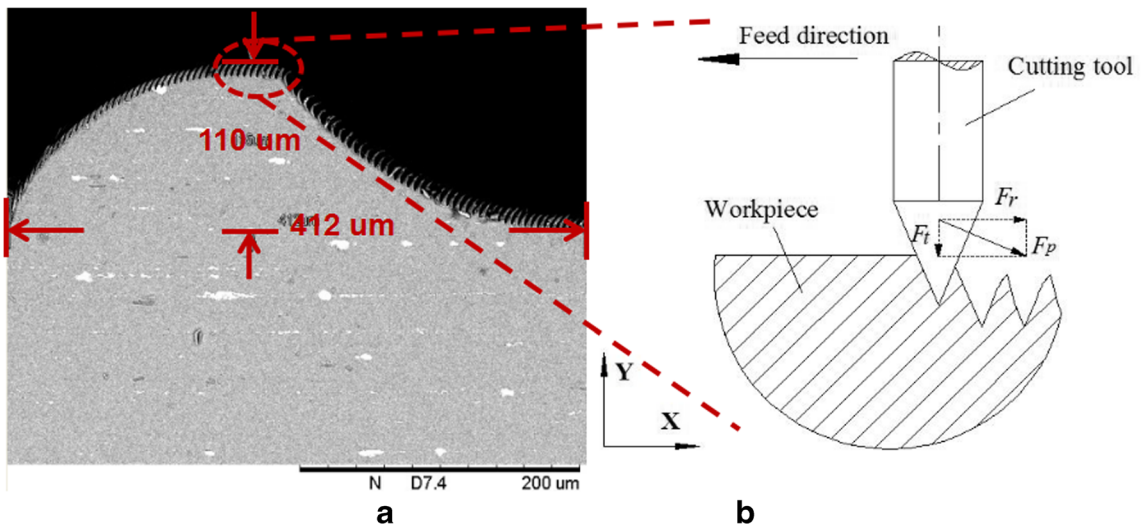

Fig. 4 The hierarchical structures. (**a**) SEM photo of a cross-section of a micro-groove cut by a sharp diamond tool, (**b**) schematic illustration of cutting force components in horizontal and vertical directions

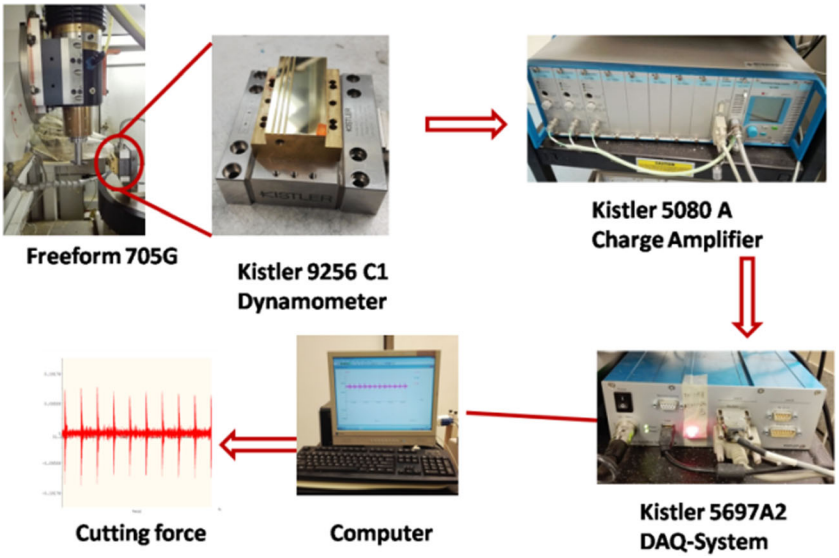

Fig. 5 Flow chart of the measurement of cutting force in UPRM

of SMVGs, to easily establish the cutting force model for this research, only the component of the cutting force in the radial direction is considered.

The cutting process is schematically illustrated in Fig. 4b, where F_p is the cutting forces perpendicular to the surface during groove formation, the force components F_r, and F_t are in the radial direction and thrust direction, respectively. The relationship is:

$$Fr = Fp \cos\frac{\alpha}{2}$$

where α is the cutting tool angle.

When the diamond tool cuts the material in a groove, the workpiece material slides along its shear plane forming chips along the rake face of the cutting tool and the F_p acts on the two sides of the groove wall. With the increase of diamond tool cutting and increase of material removal, the two edges of the diamond tool increase the pressure on both cutting surfaces in a groove. When the pressure reaches the yield of the material, the walls of the micro-grooves will deform plastically. However, the deformations of the two surfaces of a micro-groove are asymmetrical. As one side of a micro-groove is the finished surface and the other side is the transient surface, the plastic deformation will appear on the finished surfaces. In addition, the top of the grooves is thin while the root of grooves is much thicker. The radial cutting force F_r acts on the finished side wall of a micro V-groove when the force on the wall of the micro-groove exceeds the yield strength of

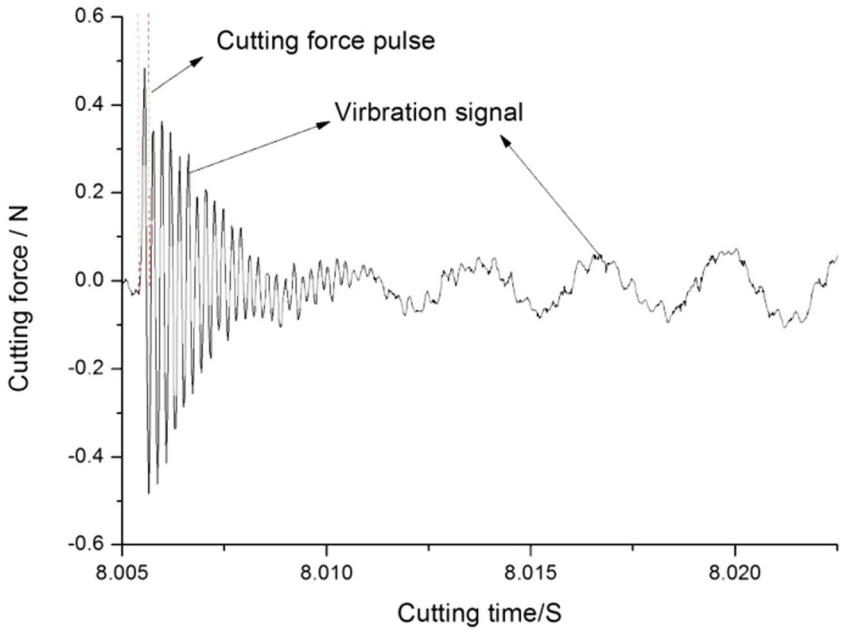

Fig. 6 The force signal of one period of the cutting process in UPRM

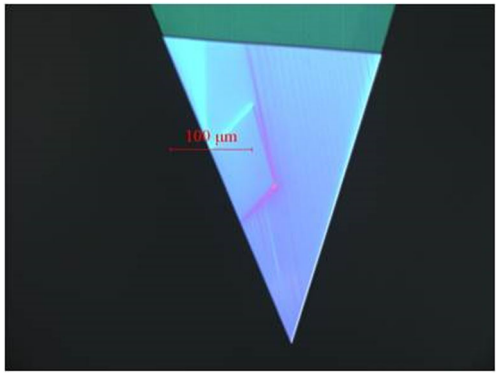

Fig. 7 Photo of a 40° single crystal diamond tool

material, and plastic deformation will appear. The mechanism of cutting radial force acting on the side wall of a micro-groove is shown in Fig. 4b.

2.2 Cutting force measurement

This paper aims to analyze the effect of cutting force under different cutting conditions on the quality of SMVGs in UPRM. The material and cutting conditions are listed in Table 1. In the cutting experiments, a multi-component dynamometer (type: Kistler 9256 C1) was employed to measure the cutting force components acting on the workpiece. A 3-channel charge amplifier (Kistler 5080A) was used to collect cutting force signals, which were converted to digital signal by using a DAQ-System (Kistler 5697A2). The acquisition system (Dynoware software) was used to describe the digital data. Figure 5 shows the setup of the measurement system.

UPRM is a typical intermittent cutting process. Therefore, the measurement of the cutting force signal is composed of the cutting force pulse component and free vibration component [13]. The cutting force pulse represents the maximum of the cutting force as shown in Fig. 6.

Because the contact time of the cutting tools with the material is very short, each cutting is a collision with the material. With regard to the effect on micro-structure, the cutting forces can be divided into radial force F_r and thrust force F_t.

2.3 Cutting condition setting

Compared with conventional NC machines, URPM has more complex and interacting machining parameters to control during machining. The machining parameters such as cutting strategy, tool path and cutting tool angle affect mostly the surface texture and form accuracy. The main cutting parameters are shown in Table 1.

The material workpiece used to investigate the effect of cutting parameters was copper. The dimension of the workpiece was 35 mm × 20 mm. Copper has very high thermal and electrical conductivity and is widely applied to manufacture heat exchangers.

This work was performed through cutting V-grooves on the copper bulk while capturing and analyzing the cutting force signals. The research investigated the effect of cutting parameters on the cutting force in UPRM. In the series of experiments, the changes of cutting force with respect to different depths of cut, spindle speed and feed rates were explored via V-groove cutting on a copper workpiece. In order to obtain steady measured results, the cutting force values were determined by solving the mean value of 100 cutting force peaks.

Diamond tools have many outstanding advantages involving nano-metric edge sharpness, high reproducibility and high wear resistance. A sharp tool whose radius of arc is extremely small is required to fabricate some special types of components, such as V-grooves. A sharp diamond tool with a 40° tool angle is shown in Fig. 7.

The angle of a SMVG is the same as the diamond tool angle, due to the principle of the one-step cutting method. The smaller the micro-groove angle is, the higher the enhancement of heat transfer that can be obtained for hierarchical micro-structure heat exchangers [3]. However, the quality of micro-grooves is very sensitive to the tool angle: the smaller the tool angle is, the harder it is to obtain a high-quality

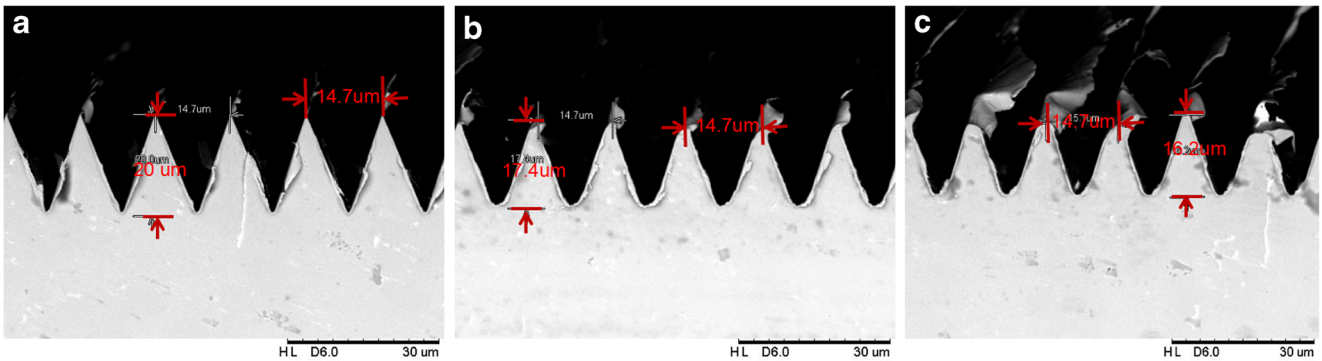

Fig. 8 SEM of cross-sectional SMVGs machined under the cutting condition of different cutting depths d: (a) $d = 2$ μm, (b) $d = 5$ μm, and (c) $d = 8$ μm

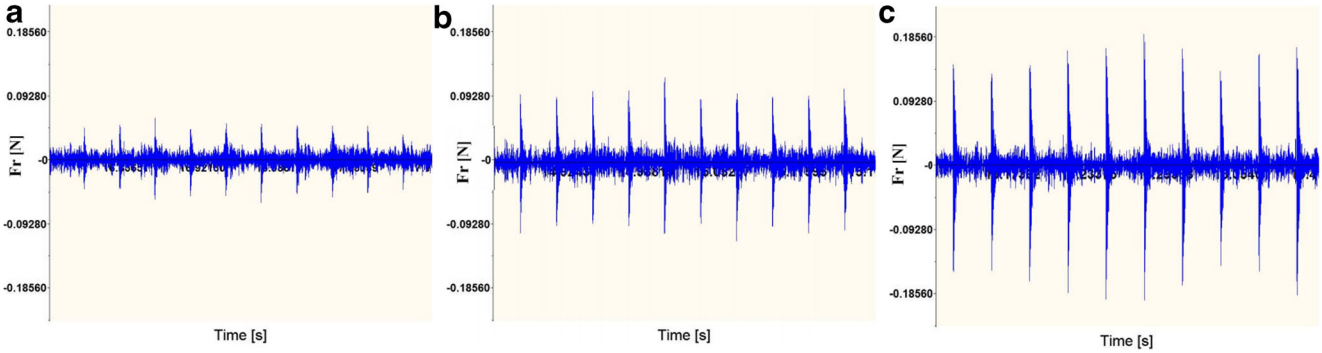

Fig. 9 The cutting force signal of F_r (**a**) $d = 2$ μm, (**b**) $d = 5$ μm, and (**c**) $d = 8$ μm

SMVGs. The hierarchical structures were fabricated on copper with different cutting conditions by UPRM.

3 Results and discussion

3.1 Effect of cutting depth

In this study, three cutting depths d were chosen: 2 μm, 5 μm, and 8 μm at the feed rate of 50 mm/min and spindle speed of 4000 rpm. The desired depth of SMVG was 20 μm. For a cutting depth of $d = 2$ μm, to achieve a micro-groove depth of 20 μm, cutting more than 10 times is needed. For $d = 5$ μm, four times are needed to achieve the desired depth. For $d =$ 8 μm, just three times is required to finish the cut. It can be clearly seen that increasing the depth of cut can greatly improve the efficiency of machining.

However, as the depth of cut increases, the volume of material removed each time increases, as does the area of contact between the tool and the material, so the cutting force also increases significantly. An increase of cutting force is often accompanied by an increase of burrs and more serious plastic deformation of the wall of micro-grooves, so the impact on SMVGs must be considered.

It can be clearly seen from Fig. 8 that a higher quality of SMVG can be obtained with a smaller depth of cut. As can be seen from Fig. 8a, a smaller cutting depth is employed to machine the SMVGs, which reduces the burrs at the top of the V-grooves, and wall deformation does not occur. Figure 8b shows the cutting depth of 5 μm; it can be seen that the burrs at the top of V-grooves increase, while the plastic deformation on the top of the wall begins to appear. The cutting depth of 8 μm is shown in Fig. 8c; it is clearly observed that the burrs at the top of the V-grooves increase very seriously and the thicker portions of the wall are also deformed.

The measured radial cutting force signals for three cutting depths 2 μm, 5 μm, and 8 μm are shown in Fig. 9 from a to c. Increase of the cutting depth leads the cutting force to grow greatly, including the thrust cutting force and radial cutting force. When the cutting depth d is 2 μm, 5 μm, and 8 μm, the mean value of radial cutting force F_r is equal to 0.07 N, 0.10 N, and 0.16 N, respectively. When the F_r exceeds the yield strength of copper, the thinner material undergoes plastic deformation. The thinner part of the V-grooves undergoes plastic deformation, and with the increase of cutting force, this deformation becomes more serious, from the top, slowly developing to the relatively thick middle part of micro-grooves.

3.2 Effect of feed rate

Under the condition where the cutting depth was 2 μm and the spindle speed was 4000 rpm, the cutting experiments were

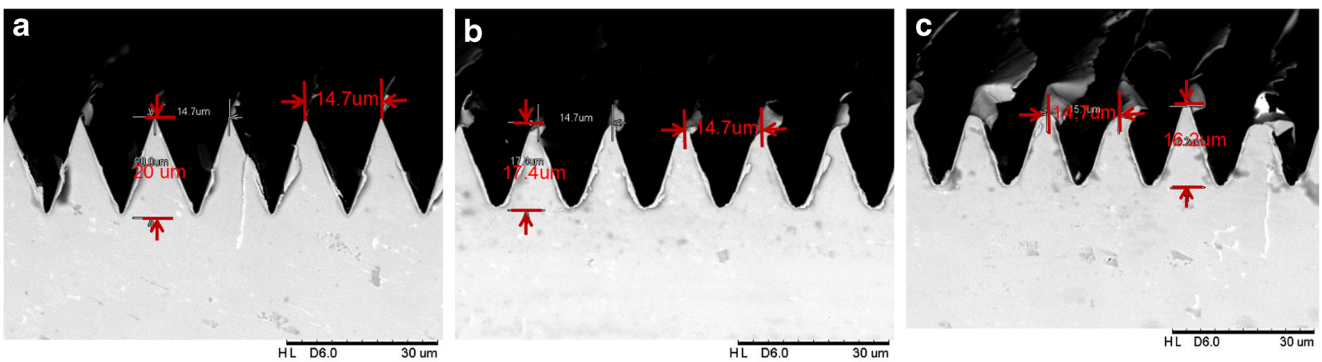

Fig. 10 SEM of cross-sectional SMVGs machined under the condition of different feed rates f: (**a**) $f = 50$ mm/min, (**b**) $f = 100$ mm/min, and (**c**) $f =$ 200 mm/min

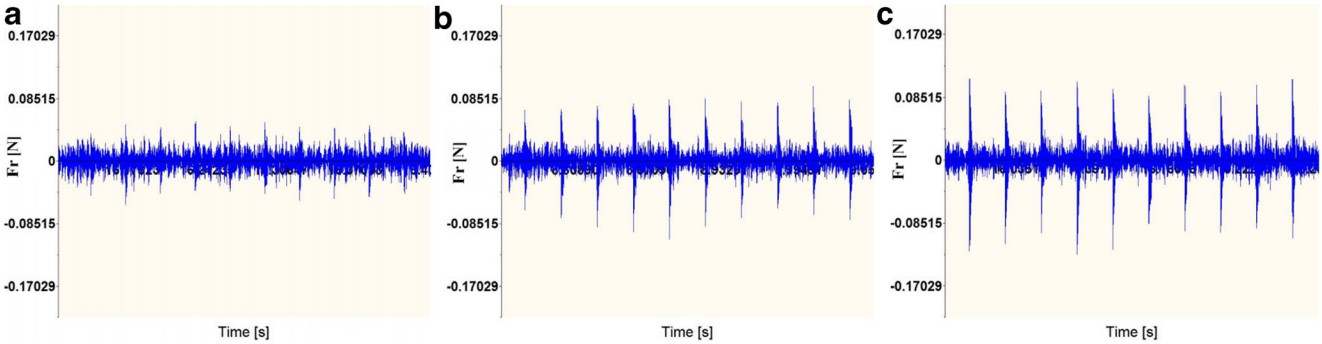

Fig. 11 The radial cutting force acting on the side wall of micro V-grooves for various feed rates: (**a**) 50 mm/min, (**b**) 100 mm/min, and (**c**) 200 mm/min

carried out with feed rates f of 50 mm/min, 100 mm/min, and 200 mm/min. Figure 10 shows the machining quality of the SMVGs with different feed rates.

It was found that the quality of SMVGs is also greatly influenced by the feed rate in the one-step machining process. The best SMVGs were obtained at $f = 50$ mm/min, which is shown in Fig. 10a. The phenomenon of burrs was not obvious at the lowest feed rate. The SEM of SMVGs machined at a feed rate $f = 100$ mm/min is shown in Fig. 10b. Burrs on the top obviously increased. The geometry of SMVGs machined at a feed rate of 200 mm/min is shown in Fig. 10a. Burrs left on the top of micro-grooves became more serious. In addition, the plastic deformation of the wall also became serious. However, the deformation was limited to the top.

Figure 11 shows the radial cutting force acting on the side wall of micro-grooves. It can be seen that increasing the feed rate causes an increase of cutting force. When the feed rate $f =$ 50 mm/min, the mean value of cutting force is 0.07 N as shown in Fig. 11a. In Fig. 11b, the mean value of cutting force is 0.09 N with feed rate $f = 100$ mm/min. Figure 11c shows the cutting force obtained at feed rate $f = 200$ mm/min. The mean value of cutting force is 0.13 N. Although increasing the value of the feed rate can greatly improve the efficiency of fly cutting for hierarchical ribs, it introduces cutting force that will not be as large as the cutting depth, and increasing the feed rate also highly influences the quality of SMVGs. Keeping a balance between fly cutting efficiency and quality of the finished micro-structure is very important.

3.3 Effect of spindle speed

In these experiments, the cutting depth was 2 μm and the feed rate was 50 mm/min. The other parameters were held constant. The SEM micrographs of the cross-section with different spindle speeds are shown in Fig. 12. As shown in Fig. 12a, the plastic deformation disappeared at the top of SMVGs. Figure 12b shows SEM photographs of micro-grooves machined at the spindle speed value of 4000 rpm. The burrs were minimized compared to when the spindle speed of 2000 rpm was applied. In addition, the deformation of the top of SMVGs disappeared. When the spindle speed was equal to 6000 rpm, deformation did not occur, and the burrs were further minimized.

Figure 13 shows the measured radial cutting force pulse acting on the side wall of micro-grooves. Increasing the spindle speed will reduce the cutting force. When the spindle speed $\omega = 2000$ rpm, the radial cutting force is 0.11 N.

From Fig. 13b, it can be seen that the radial cutting force is 0.07 N with spindle speed $\omega = 4000$ rpm. Figure 13c shows the cutting force obtained at spindle speed $\omega = 6000$ rpm. The radial cutting force is 0.05 N. So, increasing the spindle speed can obviously reduce the cutting force. With decreasing

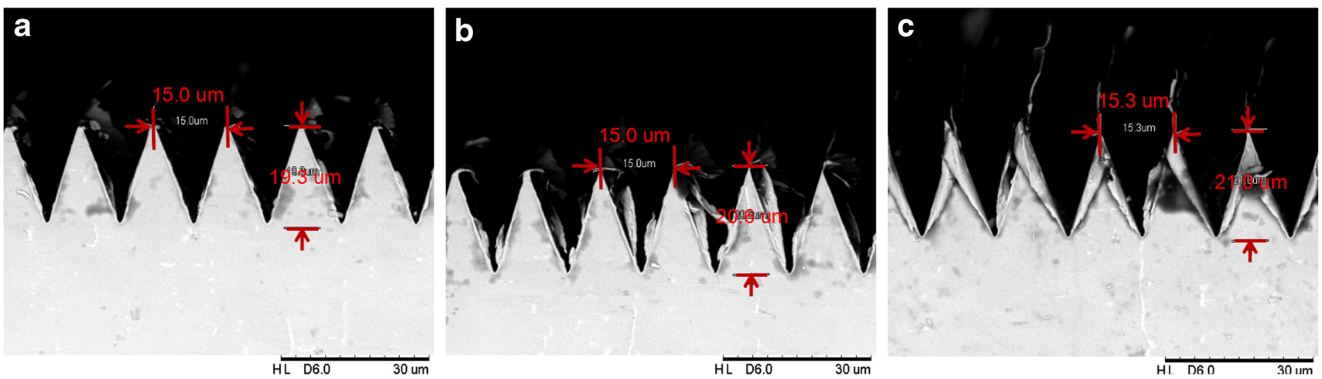

Fig. 12 SEM of cross-sectional SMVGs machined at various spindle speeds: (**a**) 2000 rpm, (**b**) 4000 rpm, and (**c**) 6000 rpm

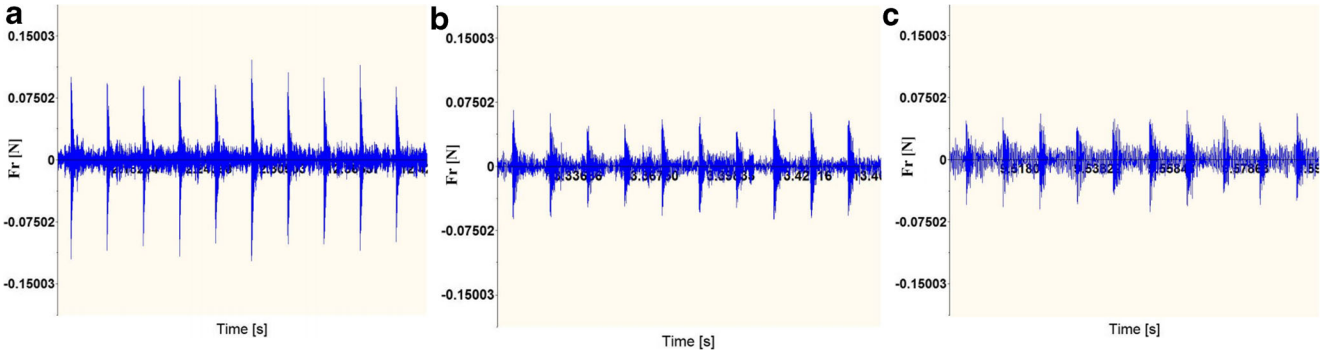

Fig. 13 The radial cutting force acting on the side wall of micro V-grooves at various spindle speeds: (**a**) 2000 rpm, (**b**) 4000 rpm, and (**c**) 6000 rpm

cutting force, no obvious plastic deformation occurs at all the tops of micro-grooves as shown in Fig. 13c.

At the same feed rate, using a higher spindle speed, the increase in the cutting times occurs at the same position. For example, at 6000 rpm, it is more than three times than at a speed of 2000 rpm. Although it can effectively reduce the cutting force produced by the plastic deformation, in regard to the removal of burrs, the effect is not very good, but at higher speed, burr residue becomes more serious.

4 Conclusions

In this paper, two items of machining defects were employed to evaluate the quality of secondary micro V-grooves of hierarchical ribs machined by one-step cutting in ultra-precision raster milling. One of them is burrs, while the other is plastic deformation of the V-groove wall. Cutting conditions can affect the removal of burrs and the amplitudes of cutting force in UPRM.

(1) A dynamometer can be used to capture a series of cutting force pulses and vibration signals in every rotary cut in UPRM. As the diamond tool cuts into and out of the workpiece, the time is very short, but the cutting force pulse can be seen as a shock, while the cutting force pulse is closely related to the plastic deformation of SMVGs.
(2) Cutting force is a series of force pulses and vibration due to the small cutting duration in every rotary cut in UPRM. As there is a crucial rotation angle that divides the chip area into two sections, the cutting force pulse is composed of two components in UPRM. The cutting force pulse is closely related to the geometric shape of cutting tools.
(3) The series of cutting experiments shows that the radial cutting force increases with growing cutting depth and feed rate, while it decreases with increasing spindle speed, and the feed rate has more influence on cutting force than cutting depth does. In addition, the burrs increase with growing depth, feed rate, and spindle speed.

Funding information The work described in this paper is partially supported by the Shenzhen Science and Technology Program (JCYJ20170818135756874) and the Shenzhen Polytechnic research Funds (no. 601822K21017).

References

1. Thianpong C, Chompookham T, Skullong S, Promvonge P (2009) Thermal characterization of turbulent flow in a channel with isosceles triangular ribs. Int Commun Heat Mass 36(7):712–717
2. Wang HT, Lee WB, Chan J, To S (2015) Numerical and experimental analysis of heat transfer in turbulent flow channels with two-dimensional ribs. Appl Therm Eng 75:623–634
3. Wang HT, Lee WB (2016) A study of cutting factors affecting the generation of functional hierarchical rib array structure in ultra-precision raster milling. Int J Adv Manuf Technol 86(1):989–998
4. Chern GL (2006) Experimental observation and analysis of burr formation mechanisms in face milling of aluminum alloys. Int J Mach Tools Manuf 46(12–13):1517–1525
5. Liu Y, Zhao W, Zhou T, Liu X, Wang X (2017) Microgroove machining on crystalline nickel phosphide plating by single-point diamond cutting. Int J Adv Manuf Technol 91(1–4):477–484
6. Juan DDCN, Jose CMV (2016) Optimization of cutting parameters to minimize energy consumption during turning of AISI 1018 steel at constant material removal rate using robust design. Int J Adv Manuf Technol 83(5–8):1341–1347
7. Mathai G, Melkote S (2012) Effect of process parameters on the rate of abrasive assisted brush deburring of microgrooves. Int J Mach Tools Manuf 57:46–54
8. Saglam H, Unsacar F, Yaldiz S (2006) Investigation of the effect of rake angle on main cutting force and tool tip temperature. Int J Mach Tools Manuf 46(9):132–141
9. Wu X, Li L, He N (2017) Investigation on the burr formation mechanism in micro cutting. Prec Eng 47(1–4):191–196
10. Fernando BO, Alessandro RR, Reginaldo TC, Adriano FS (2015) Size effect and minimum chip thickness in micromilling. Int J Mach Tools Manuf 89:39–54
11. Bissacco G, Hansen HN, Chiffre L (2005) Micromilling of hardened tool steel for mould making applications. J Mater Process Technol 167:201–207

12. Schueler GM, Engmann J, Marx T, Haberland R, Aurich JC (2009) Burr formation and surface characteristics in micro-end milling of titanium alloys burrs-analysis, control and removal. Proc CICB, pp: 129–138
13. To S, Zhang GQ (2014) Study of cutting force in ultra-precision raster milling of V-groove. Int J Adv Manuf Technol 75:967–978
14. Parsa MH, Nasher AAS, Ettehad M (2010) Experimental and finite element study on the spring back of double curved aluminum/polypropylene/aluminum sandwich sheet. Mater Design 31(9): 4174–4183
15. Guo P, Lu Y, Ehmann KF, Cao J (2014) Generation of hierarchical micro- structures for anisotropic wetting by elliptical vibration cutting. CIRP Ann Manuf Technol 63(1):553–556
16. To S, Zhu ZW, Wang HT (2016) Virtual spindle based tool servo diamond turning of discontinuously structured microoptics arrays. CIRP Ann Manuf Technol 65(1):475–478